MATERIALE PLASTICE
https://revmaterialeplastice.ro
https://doi.org/10.37358/Mat.Plast.1964

Physico-chemical Characterization of Paint Films with Electromagnetic Properties

ALINA RUXANDRA CARAMITU[1], IOANA ION[1], ADRIANA MARIANA BORS[2*], CRISTIAN ROMEO CIOBANU[3], CRISTINA SCHREINER[3], MIHAELA ARADOAEI[3], ANA-MARIA DANIELA CARAMITU[4]

[1]National Research and Development Institute for Electrical Engineering INCDIE ICPE - CA Bucharest, 313 Splaiul Unirii, 030138, Bucharest, Romania
[2]ICPE S.A. Bucharest, 313 Splaiul Unirii, 030138, Bucharest, Romania
[3]Gh. Asachi Technical University of Iași, 67 Prof. dr. doc. Dimitrie Mangeron Str., 700050, Iasi, Romania
[4]Medlife S.A. Bucharest, 365 Calea Grivitei, 010719, Bucharest, Romania

Abstract: *Electromagnetic compatibility issues and those generated by these radiations are a major concern for electrical and electronic products, mainly in the fields of communications, information technology, transportation, security and medical services. The paper presents the way to obtain nanostructured paint/plastic/nanopowder paint systems with electromagnetic shielding properties, as well as their characterization by FTIR analysis, DSC and dielectric tests. These systems have Electromagnetic Interference (EMI)/Electromagnetic Compatibility (EMC) and Electrostatic Discharge (ESD) applications in the manufacture of enclosures for various electronic devices and for the automotive industry. At the laboratory level, 4 non-additive experimental models (EM) coded M1-M4 and 16 additive experimental models coded M5-M20 were obtained. Revolutionary to these materials is the fact that inside they are insulating and, on the outside, they behave like a shield. The results obtained from the dielectric tests performed on the 16 additive systems showed that the samples with a maximum percentage (20 %) of metal nanopowders show the highest values of electrical conductivity. Of the two nanopowders used, that of Fe from samples M11, M12, M19 and M20 which induces the composite higher conductivities than Al nanopowders. The ATR/FTIR spectra of the two paint samples analyzed showed that they were almost identical, suggesting that the paints tested had the same basic chemical structure. DSC analysis showed that pigment paint (V2) has low thermal oxidation stability and lower decomposition temperatures than pigment-free paint (V1), therefore, V2 is less stable under usage conditions, under the influence of normal environmental factors (temperature, humidity, natural or artificial light, etc.) compared to V1.*

Keywords: *nanostructured paint, nanopowder, composite materials, electromagnetic shielding, conductivity*

1.Introduction

The anti-corrosive properties of paints have been extensively studied [1-3] and it has been found that there are also paints that have the effect of shielding electromagnetic radiation. New materials such as paints with a role in both, the combination of building materials and the increase of the effectiveness of shielding are of real interest as proven by the specialized literature [4-9]. From simple instruments and devices, mankind has gradually evolved towards various, much more technically complicated innovative devices.

As a result, there is a steady increase in electromagnetic fields, which are almost impossible to avoid. Electromagnetic radiation affects not only the technical devices but also the human body, the biological effects depending on the type, frequency and intensity of these fields [5]. The presence of many sources of electromagnetic radiation can be a problem in television broadcasts, military and medical applications.

**email:adriana.bors@icpe.ro; adrianambors@gmail.com*

In this context, many researchers are currently focusing on the development of materials and structures that have the ability to effectively protect against electromagnetic waves. The aim is to reduce the amount of radiation that passes from the outside to the inside of the building [10,11] and to minimize the effects of this radiation on the human body [12]. Materials that absorb electromagnetic radiation can be produced in a variety of shapes, such as paints, sheets, and thin films [13-16]. Depending on the electromagnetic properties, the material can be used either as an absorber or as a reflector of electromagnetic radiation [17-19]. Absorbent materials can be grouped into two categories: resonant (or narrowband) and broadband. Resonant materials are more common, while broadband materials are produced by combining different materials [20]. The absorption obtained depends on the thickness and the absorption mechanisms, which are independent of one another. By choosing a suitable thickness, the absorption bandwidth can be considerably increased, both at the normal and oblique incidence of the electromagnetic wave [5, 19-22]. Electromagnetic compatibility is a field of actuality, being imposed by the development of electronics, especially high speed and low consumption applications, nonlinear electrical engineering, expansion and diversification of communication and data transmission networks, increasing the degree of interconnection within energy networks but also of another nature. All this has led to an increase in the degree of electromagnetic pollution both in the environment and in all energy, communications or other networks [6]. Most paints on the market with electromagnetic shielding effect use carbon or metals to block radio frequencies. When radiation hits the reflective material, it moves away from the surface. Popular brands of RF blocking paint include Y-shield, CuPro-Cote, EMF-Turtal, Aegis Guard and Geovital T-98. Thus, Yshield is a conductive paint based on graphite and carbon and offers very high levels of protection against radiation and RF shielding. The manufacturer claims that with three coats of paint it gets a reduction of up to 59 dB which means that the paint blocks 99.9999 % of the radio frequencies. CuPro-Cote is an EMF blocking paint made of copper. Copper paint has a low VOC content, is non-toxic and easy to clean. The manufacturer claims to achieve an attenuation of "more than 75 dB from 30 MHz to 1.5 GHz". EMF-Turtal is a paint based on graphite and graphene powder. EMF-Turtal claims to effectively block 40GHz "5G" millimeter waves up to 64 db with two layers. Aegis Guard EMF has no metals in it. It is an acrylic paint with various additives that deflects electrical signals up to 5G of 300 GHz, 600 GHz and the future 6G 1 THz and has applications in RF and EMF shielding. Geovital T-98 EMF is a water-based acrylic paint containing graphite and additives and "absorbs" up to 15 % of the radio frequency, so it is less deviated by paint. T-98 claims to achieve an attenuation of up to 50 dB (99.999 %) with frequencies of up to 10 Ghz in two layers. In this context, the main objective of this paper was to produce and characterize broadband radar absorbing material (RAMs) in the form of paints to absorb electromagnetic radiation. For this it was used an acrylic paint in which it was introduced separately Al nanopowders and Fe nanopowders. Thus, 20 paint/plastic/Al and Fe nanopowder systems coded M1-M20 were made. Various additives have been introduced in the composition of the paint to improve the display on plastic holders. Additives were tested for *p*H change (CH_3COOH for acidic medium and NaOH for basic medium, respectively) as well as for improving dispersion, by treatment with stabilizing/coating agents such as (sodium dodecyl sulfate) SDS and (polyviniylpyrrolidone) PVP. Additives for changing the *p*H have led to precipitation of the samples. From the 2 additives, SDS and PVP, respectively, SDS was chosen because its use leads to a slight increase in the electrical conductivity of the samples. Thus, of the 20 EM made, M1-M4 are non-additive and M5-M20 are additive. All EMs were characterized by dielectric and FTIR and DSC analysis.

2.Materials and methods

The raw materials used have low prices and are easy to find on the market. Nanostructured paint/ plastic/nanopowder paint systems with electromagnetic shielding properties were obtained from them.

The equipment used for the characterizations were: SOLARTRON dielectric spectrometer, from Solartron Analytical, purchased in 2010, Jasco FT-IR 4200 spectrophotometer, from Jasco Ind purchased in 2007, USC - T type VWR ultrasonic bath, lamp Mercury HGW 160W / 27 230-240V Hungary 1004 and Differential Scanning Calorimeter DSC UV.

2.1. Obtaining composite materials

For a good display of the paint on the surface of the samples, it was performed according to [20]. EM of paint/plastic/nanopowder systems are made of unsanded plates treated with the 2 paints V1 and V2. The supports are immersed in paint/nanopowder/additive systems.

2.2. Preparation of nanopowder filling and additives

Due to the nanopowders agglomeration, they were ultrasounded in a USC - T type VWR ultrasonic bath for 30 min. This ultrasonic bath is necessary to break up the agglomerations of nanopowders used in the first stage when mixing the nanopowders with additive and water for 5 min and then after introducing the mixture into the paint for another 30 min.

2.3. Paint preparation

The studied paints, coded with V1 and V2 were prepared with a 5 % dilution for the first layer and in the second undiluted layer, according to the product data sheet [20]. Display of the first and second coat of paint - the paint layers are spread on the surfaces of the samples only after pickling (cleaning them of dust with a dry cloth) and degreasing them with acetone.

2.4. Work way for additive

Additive - this step is necessary because the in-homogeneity of the powders in the paint mass has been found. In order to choose the optimal additive, several additive variants were tried. The MS chosen for the selection of the additive were M5 and M6, respectively the recipes with white paint and 10 % Al nanopowder. Thus, an add-on was attempted by:

- changing the *p*H:

-*p*H acid - by adding 1mL acetic acid 40 % concentration. Thus, the composition was composed of: 1ml acetic acid + 5 g nanopowder of Al + 45 g V1 coded paint - it is found that the paint precipitated;

-*p*H basic - by adding 100 mg NaOH + 5 g nanopowder of Al + 45 g V1 coded paint described above in point a - it is found that the paint has precipitated;

- dispersion with:

- SDS (sodium dodecyl sulfate)- the composition was composed of: 0.5 g SDS + 5 g nanopowder of Al + 45 g V1 coded paint, foaming is observed;

- PVP (polyvinyl pyrrolidone)- the composition was composed of: 0.5 g PVP + 5 g nanopowder of Al + 45 g V1 coded paint, the best homogeneity is observed.

3.Results and discussions

The raw materials needed to obtain the proposed experimental models consisted of:

- Oskar Direct Paint on Melamine and White Coconut Plastic 0.6l coded with V1
- Oskar Direct paint on Melamine and Plastic Silver 0.6l coded with V2

Table 1. Main features of paints [19]

No. crt.	Characteristic	Unit	Value	Analysis method
1	Appearance	-	homogeneous, viscous liquid, free of impurities	visual
2	Density, 20ºC	g/cm^3	1.1-1.26 ± 0.02 depending on the product	SR EN ISO 2811: 2016 P1
3	Viscosity as run off time (6 mm, 20ºC)	s	40-80 color function	SR EN ISO 2431:2012
4	Coverage power, min		min. 96.00	IL-QC-20

- Plate support: Guttagliss Hobbyglas, transparent, 1000x500x2 mm and Gutta Hobby color, white, 500x500x3 mm

- The fillers/reinforcers used were Al and Fe nanopowders purchased from NANOGRAFI LTD.STI, Ankara Turkey [7] with the particle size shown in [8] for the two powders.

The equipment used for the characterizations were: SOLARTRON dielectric spectrometer, from Solartron Analytical, purchased in 2010, Jasco FT-IR 4200 spectrophotometer, from Jasco Ind purchased in 2007, USC - T type VWR ultrasonic bath, lamp Mercury HGW 160W / 27 230-240V Hungary 1004 and Differential Scanning Calorimeter DSC UV.

3.1. Obtaining composite material systems and coding of evidence

The samples were obtained by immersing the supports in the mixtures of paint/nanopowders/ additives. Thus, the experimental models M1 and M2 displayed with V1 and M3 and M4 displayed with V2 were obtained to obtain the other experimental models, 10 and 20% nanopowders of Al and Fe with a granulation of 800 nm were introduced in the paint composition.

Table 2. Coding of composite material samples

M1 transparent support (coded T) + V1;	M11 T + V1 + SDS + 20 % Fe nanopowder;
M2 white support (coded A) + V1	M12 A + V1 + SDS + 20 % Fe nanopowder;
M3 T + V2	M13 T + V2 + SDS + 10 % Al nanopowder;
M4 A + V2	M14 A + V2 + SDS + 10 % Al nanopowder;
M5 T + V1 + SDS + 10 % Al nanopowder;	M15 T + V2 + SDS + 20 % Al nanopowder;
M6 A + V1 + SDS + 10 % Al nanopowder;	M16 A + V2 + SDS + 20 % Al nanopowder;
M7 T + V1 + SDS + 20 % Al nanopowder;	M17 T + V2 + SDS + 10 % Fe nanopowder;
M8 A + V1 + SDS + 20 % Al nanopowder;	M18 A + V2 + SDS + 10 % Fe nanopowder;
M9 T + V1 + SDS + 10 % Fe nanopowder;	M19 T + V2 + SDS + 20 % Fe nanopowder;
M10 A + V1 + SDS + 10 % Fe nanopowder;	M20 A + V2 + SDS + 20 % Fe nanopowder;

3.2. Characterization of paint/plastic/nanopower and additive systems

The dielectric tests are performed on the SOLARTRON impedance analyzer according to the working instruction IL MAv - 06, edition 1 update 0 /10.2017. The technical characteristics of this analyzer are:

- temperature range: -269 ... + 400°C;
- temperature rise rate (heating / cooling) 0.01 - 30°C / min; thermal stability: max ± 0.01°C;
- frequency range: 10 μHz ..... 20 MHz;
- loss factor range: 10^{-4} ... 10^{3};
- thermal stabilization: max. 8 min;
- data acquisition software: Smart.

The device may cause:

- real relative permittivity;
- imaginary relative permittivity;
- tangent of the dielectric loss angle;
- capacitance;
- electrical impedance and admittance.
- The tests were performed in air at a voltage of 1 V and the frequency range 1-10 kHz. The samples were pleasantly squared shaped with a side of 30 mm and a thickness of 2 mm for the transparent support and 3 mm for the white support, respectively.
- The electrical conductivity was calculated according to the formula:
-

$$\sigma = 2\pi f \varepsilon_o \varepsilon_r \, tg\delta \quad (1)$$

$\omega = 2\pi f$ angular frequency
ε_o = air permittivity (8.85 x 10-12 Fm^{-1})
ε_r – real permissiveness
$tg\delta$ – tangent of the dielectric loss angle.

The dielectric tests were performed in several conditions in order to be able to choose the optimal variant of obtaining the paint/plastic/nanopowder systems. Thus, dielectric tests were performed on the sandblasted, additive and non-additive samples, as well as on non-sandblasted samples, in order to be able to choose the optimal dispersion method.

3.3.Non-adivate materials

Non-adivate materials are M1, M2, M3 and M4, ie materials displayed only with paint.

Figure 1 shows that the non-additive materials M1, M2, M3 and M4 have similar conductivities. M2 has a 19 % higher electrical conductivity than M1, 21 % higher than M3 and 20 % higher than M4.

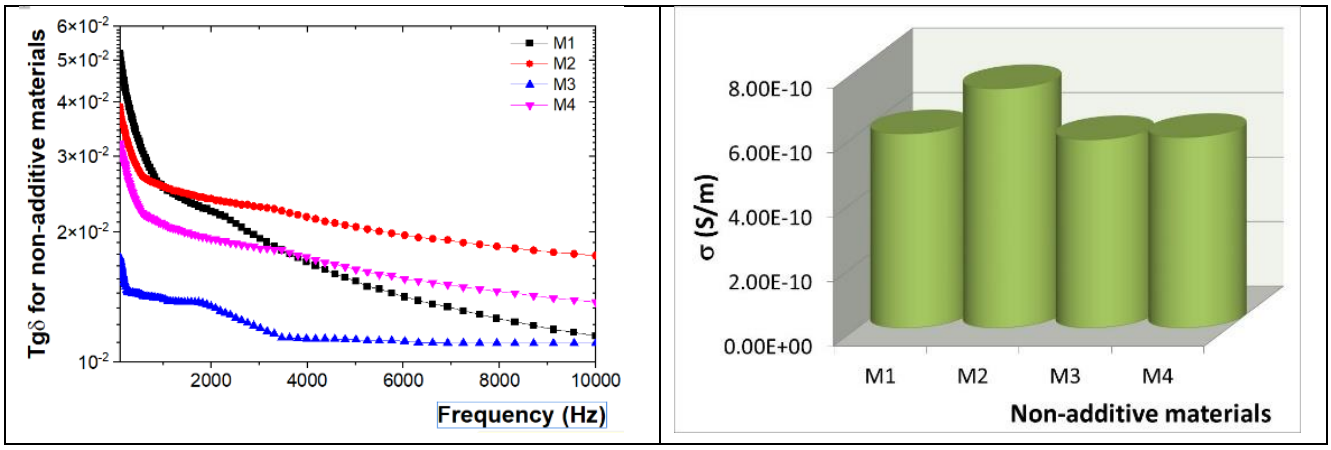

(a) (b)

Figure 1. Variation (a) tg δ frequency function for non-additive materials and of (b) σ electrical conductivity of non-additive materials

3.4.Non-additive materials aged with UV radiation

Non-additive EMs (M1-M4) were subjected to 72 h UV radiation cycles for a duration of 360 h on a Mercorlux Blacklight (UV) Mercury HGW 160W/27 230-240V Hungary 1004 UV lamp with a dose of 150 mW/m^2 per hour at a temperature of 40^{o}C and humidity of 60 %.

Table 3 shows the average variation of tgδ, σ and ρ, as well as their variations for each aging cycle due to the action of UV radiation.

Table 3. Average values of the loss tangent (tg δ), electrical conductivity (σ), and electrical resistivity (ρ) for each cycle of UV irradiation

Sample	Tgδ	σ (S/m)	ρ (Ωxm)
M1	6.33E-02	1.99E-05	5.04E+04
M2	2.30E-01	3.00E-05	3.33E+04
M3	3.38E-02	2.05E-05	4.88E+04
M4	5.57E-02	2.64E-05	3.79E+04
M1 72 hours	3.30E-02	2.22E-05	4.51E+04
M2 72 hours	5.03E-02	5.94E-05	1.68E+04
M3 72 hours	3.28E-02	2.02E-05	4.94E+04
M4 72 hours	5.22E-02	5.75E-05	1.74E+04
M1 144 hours	3.47E-02	2.09E-05	4.78E+04
M2 144 hours	5.36E-02	2.73E-05	3.66E+04
M3 144 hours	3.42E-02	2.06E-05	4.85E+04
M4 144 hours	5.63E-02	2.70E-05	3.70E+04
M1 216 hours	3.62E-02	2.14E-05	4.67E+04
M2 216 hours	5.94E-02	2.96E-05	3.38E+04
M3 216 hours	3.77E-02	6.77E-06	1.48E+05
M4 216 hours	6.01E-02	2.92E-05	3.42E+04
M1 288 hours	3.27E-02	1.97E-05	5.07E+04
M2 288 hours	5.35E-02	2.74E-05	3.64E+04

Sample	Tgδ	σ (S/m)	ρ (Ωxm)
M3 288 hours	3.42E-02	2.08E-05	4.80E+04
M4 288 hours	5.51E-02	5.44E-06	1.84E+05
M1 360 hours	3.26E-02	2.38E-05	4.20E+04
M2 360 hours	5.75E-02	2.95E-05	3.38E+04
M3 360 hours	3.72E-02	2.34E-05	4.27E+04
M4 360 hours	5.65E-02	2.80E-05	3.57E+04

The experimental data obtained show that the tgδ, decreases after the first two doses of UV irradiation (72 and 144 h) which indicates that the polymerization has not been completed. In the interval of 144 - 360 h of UV radiation, a slight increase of the tgδ, is observed, which indicates a beginning of the decrease of the coating capacity and implicitly a degradation of the paint / coating layer. The decrease in tg δ is associated with the increase σ, which is justified by the fact that the paint layer begins to show micro-cracks (unnoticeable to the naked eye). For M1-M4, it was calculated the estimated remaining lifetime in case exposure to UV radiation was continued. The critical value of the electrical resistivity at which the material can be considered degraded was chosen as the moment when the electrical resistivity decreases to 30% of the initial value. Using the formulas for calculating the root of the equation of degree 2 given by the graph we obtain the data from Table 3. Thus, we can identify the number of hours of UV irradiation supported by the material until aging. For materials used in industry, this value can determine the shelf life of the material and implicitly when it should be replaced. Following the calculations made to determine the remaining life, it was found that (Table 4) the coatings should be redone before the irreparable damage to the covered areas is reached.

Table 4. Calculation of the remaining life until the critical value is reached in case of exposure to UV radiation

Sample	Equation	y	Intercept	y-Intercept=C	B1 (b)	B2 (a)	Δ	Remaining life time (h)	Calculated lifetime until remediation (h)
M1	$y-C-B1x-B2x^2=0$	1.00E+04	2.77E+04	-1.77E+04	-1.13E+02	6.60E-01	5.96E+04	118	478
M2		1.51E+04	4.86E+04	-3.35E+04	-7.34E+00	7.52E-03	1.06E+03	0	360
M3		1.46E+04	3.43E+04	-1.96E+04	5.52E+02	-1.46E+00	1.90E+05	85	445
M4		1.14E+04	1.60E+04	-4.61E+03	3.39E+02	-4.06E-01	1.07E+05	2	362

These estimates indicate that the M2 material must be resurfaced after a minimum of hours (360 h) and the M1 material must be resurfaced after the maximum of hours has been reached (445 h). So, the most affected by UV radiation is M2 and the most resistant to UV radiation is M4.

3.5.Additive selection

Dielectrically tested additive materials are M5 and M6 additive with SDS and compared to additive with PVP. These samples are coded as follows: M5 SDS, M6 SDS, M5 PVP and M6 PVP.

The experimental results obtained by mediating 200 values are presented in Table 5.

Table 5. Electrical conductivity for additive samples

EM	σ
M5	2.39E-10
M5 SDS	7.15E-10
M5 PVP	6.81E-10
M6	5.64E-10
M6 SDS	7.37E-10
M6 PVP	5.94E-10

It is found that the addition with SDS (Table 4) induces an increase in electrical conductivity for both materials tested, which leads us to the conclusion that the addition with SDS is optimal.

The advantage of adding with SDS is the increase in electrical conductivity by about 5 and 20% respectively for M5 and M6 materials, respectively, and the disadvantage of this addition is the difficulty of displaying a uniform film on the support due to the foaming effect.

The advantage of PVP additive is a good display of the film on the surface of the support, and the disadvantage is that σ is smaller than that of the SDS additive material.

SDS additive materials

- V1 + T/A type materials + Al nanopowder

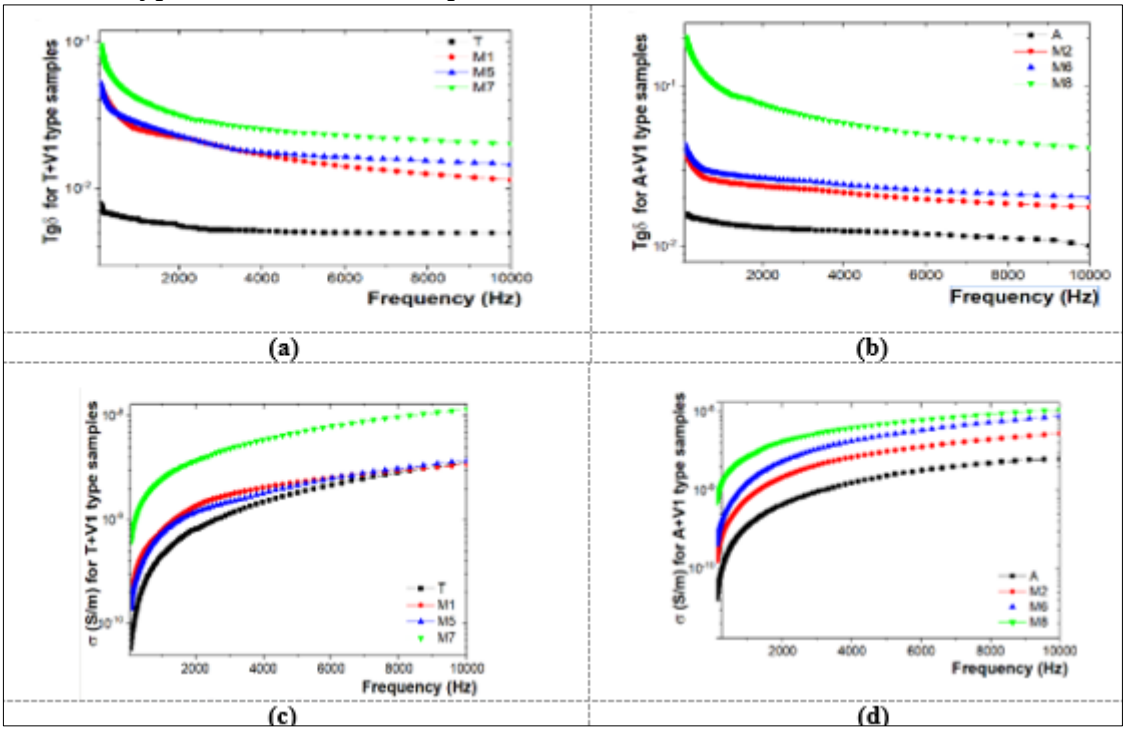

Figure 2. Variation tg δ and σ as a function of frequency for materials reinforced with Al nanopowders of type (a) and (c) T + V1 and (b) and (d) A + V1

Figure 2a, b shows that the order of increase of tgδ is T<M1<M5<M7 and respectively A<M2< M6<M8. The electrical conductivities (Figure 2c, d) also vary in the same direction thus, the highest conductivity is presented by the materials M7 and M8, respectively, which is perfectly justifiable by the fact that these two materials have a content of 20% in Al nanopowder.

- V1 type materials + T / A + Fe nanopowder

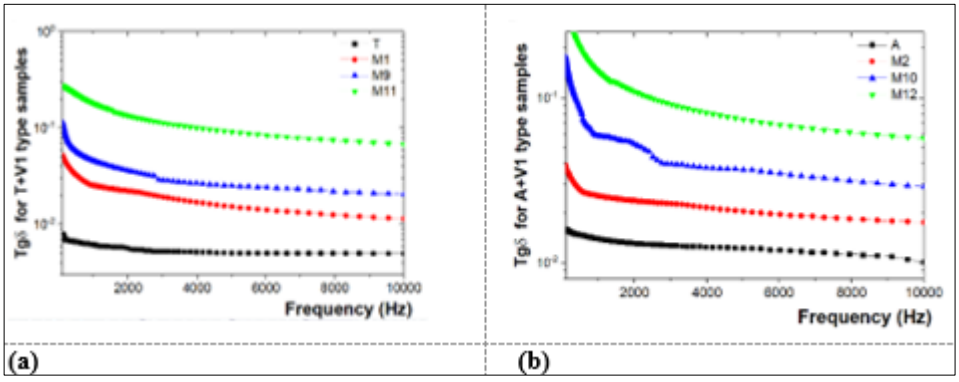

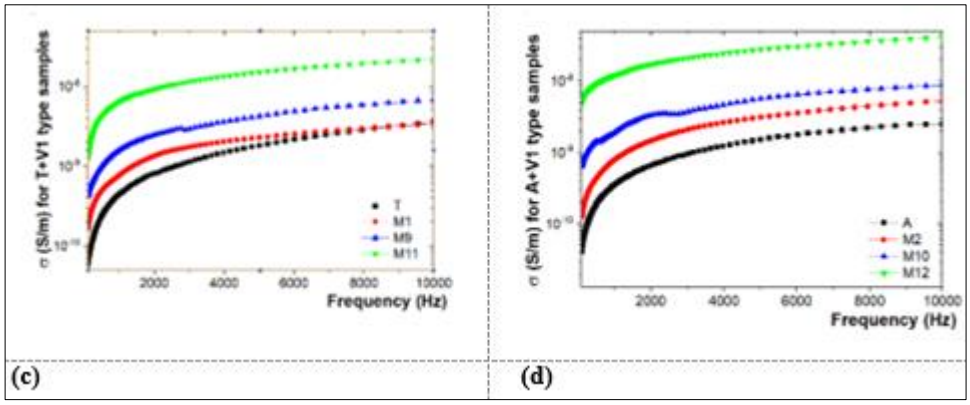

Figure 3. Variation tg δ and σ as a function of frequency for materials reinforced with Fe nanopowders of type (a) and (c) T + V1 and (b) and (d) A + V1

In the case of materials M9, M10, M11 and M12 the direction of increase of tgδ and σ is the same as in the case of materials M5, M6, M7 and M8. Figure 3a and b show the same direction of increase, the order of increase of tgδ is T<M1<M9<M11 and respectively A<M2<M10<M12.

The electrical conductivity (Figure 3 c, d) varies in the same direction, so the highest conductivity is presented by the materials M11 and M12, respectively, which is perfectly justified by the fact that these two materials have a content of 20% in Fe nanopowder.

- V2 type materials + T/A + Al nanopowder

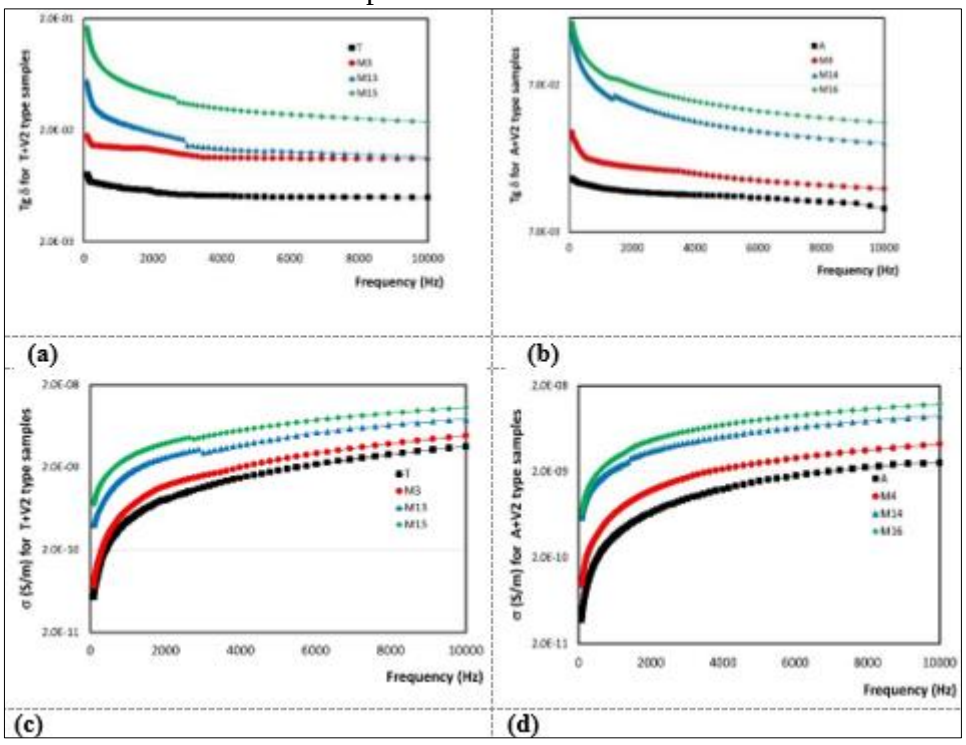

Figure 4. Variation tg δ and σ as a function of frequency for materials reinforced with Al nanopowders of type (a) and (c) T + V2 and (b) and (d) A + V2

Figure 4 a and b show the order of increase of tgδ, namely, T<M3<M13<M15 and A<M4<M14 <M16, respectively. The electrical conductivities (Figure 4 c and d) vary in the same direction.

Thus, the highest conductivity is presented by the materials M15 and M16, respectively, and in this case the higher conductivity is due to the higher concentration in nanopowder of Al.

- V2 type materials + T/A + Fe nanopowder

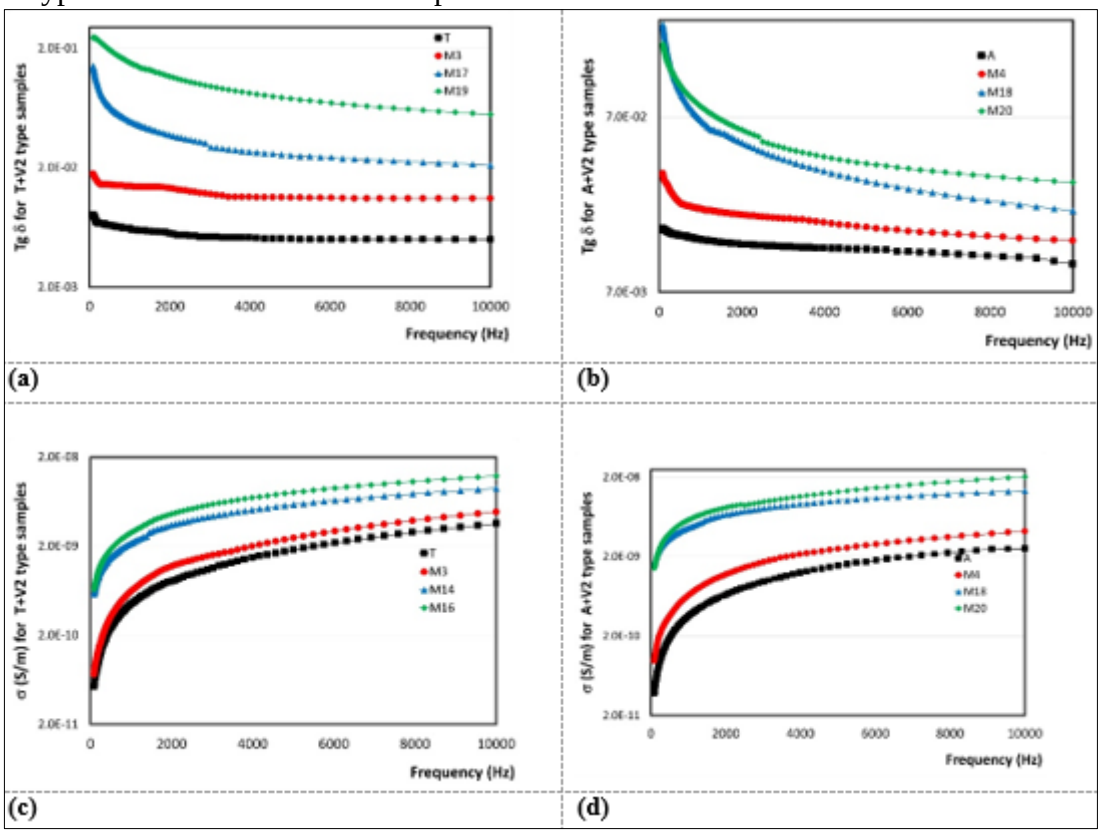

Figure 5. Variation tg δ and σ as a function of frequency for materials reinforced with Fe nanopowders of type (a) and (c) T + V2 and (b) and (d) A + V2

In the case of materials with fillings of Fe nanopowders, the same sense of variation of the parameters tgδ and σ is found. Figure 6 shows the variation of electrical conductivity in all tested materials. It is found that M11, M12, M19 and M20 have the highest values of electrical conductivity.

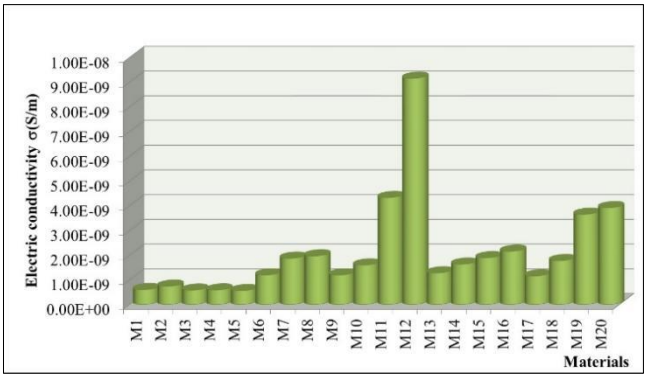

Figure 6. Electrical conductivity of the studied materials

3.6. Conclusions from dielectric tests

In this paper, dielectric tests were performed on 20 EM added and non-added, at the same time dielectric tests were performed on non-added experimental models and subjected to UV radiation for 360 h. From the comparative analysis of the experimental results obtained for tg δ and from the calculation σ for the 20 obtained systems it can be said that the materials M11, M12, M19 and M20 have the highest value of electrical conductivity.

This is explained by the addition of 20 % Fe nanopowder in the system composition.

Following the calculations made to determine the remaining life, it was found that the coatings should be rebuilt before the irreparable damage to the covered areas is reached.

3.7. FTIR analysis

The FTIR spectra of the paint samples were recorded with a Jasco 4200 spectrometer coupled with an accessory - ATR (Attenuated Total Reflectance) JASCO PRO 470-H. The samples were measured directly by placing them and pressing with a controlled force on the crystal of the ATR device.

The conditions for recording the spectra were as follows:

- spectral range: 4000 - 500 cm^{-1};
- resolution: 4 cm^{-1};
- number of spectra: 50 accumulations.

Figure 7 shows the ATR / FTIR spectra recorded on the two paint samples analyzed.

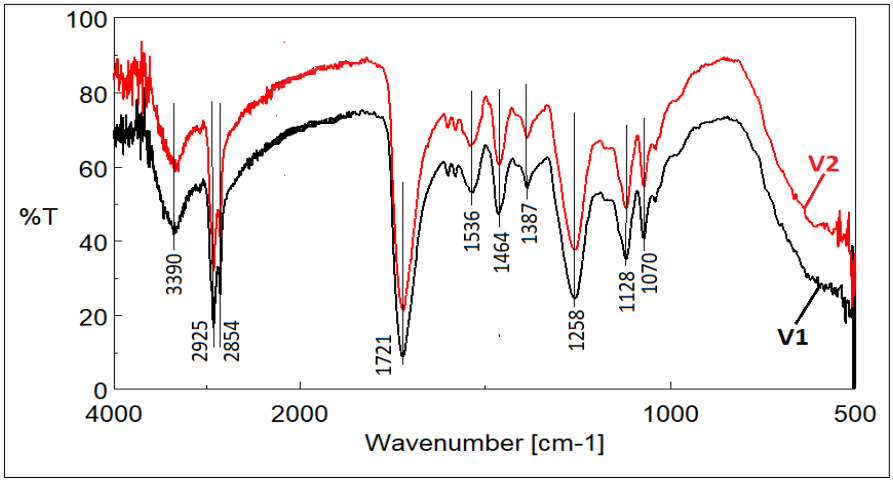

Figure 7. ATR/FTIR spectra recorded on the analyzed paint samples

The spectra show absorption bands characteristic of different functional groups existing in the chemical structure of the analyzed samples, as follows [22]:

- 3100-3600 cm^{-1}, with a maximum at about. 3390 cm^{-1}, characteristic of the stretching vibration of hydroxyl groups (-OH);
- 2700-3000 cm^{-1}, characteristic of the tensile vibrations of the -CH type groups: 2951 and 2925 cm^{-1} (asymmetric tensile vibration CH_3), 2854 cm^{-1} (tensile vibration CH_2);
- 1610-1780 cm^{-1}, band characteristic of carbonyl groups; has a main maximum at about 1721 cm^{-1} (due to stretching vibration of the C-O group) and a secondary maximum at about 1715 cm^{-1} (due to vibration type ketone -C=O);
- 1500-1570 cm^{-1}, with maximum at about 1536 cm^{-1}, characteristic of vibration -C= O;
- 1430-1500 cm^{-1}, with a maximum at about 1464 cm^{-1}, due to C-H bending vibrations (CH_2, CH_3);
- 1330-1420 cm^{-1}, with maximum at about 1387 cm^{-1}, characteristic of symmetrical deformation of CH_2
- 1258 cm^{-1}, characteristic C-O-C ester type 1000-1180 cm^{-1}, band with several maxima (1040, 1070 and 1128 cm^{-1}, respectively) characteristic of different modes of vibration of the C-O group;
- 1000-1180 cm^{-1}, band with several maxima (1040, 1070 and 1128 cm^{-1}, respectively) characteristic of different modes of vibration of the C-O group.

The high intensity peak from 1258 cm^{-1}, as well as the doublet from 1128 cm^{-1} and 1170 cm^{-1} are characteristic of acrylic type compounds [23]. Correlating these data with the fact that the bands in the regions 2700-3000cm^{-1}, 1610-1780cm^{-1} and from 1430-1500cm^{-1}, are characteristic of methyl-methacrylate compounds [24], it can be concluded that the two types of paints analyzed are acrylic type.

The other peaks observed in the FTIR spectra may be due to additives in the paint of an organic or inorganic nature, to the type of color pigments, or to metal oxides used to improve the properties of adhesion, drying and stability under usage conditions. To confirm the presence of these additives, it is necessary to use complementary analysis techniques (such as Raman spectroscopy, SEM, XRD, XRF, etc.).

As shown in Figure 13, the ATR/FTIR spectra of the two samples are almost identical, suggesting that the two paints analyzed have the same basic chemical structure. Although there are color differences between the two paints, white (V1) and silver (V2), respectively, the ATR/FTIR spectrum of sample V2 does not show additional bands to be attributed to the color pigment. This aspect can be explained by the fact that the pigment used in V2 does not absorb into IR (such as metal powders), or is very weak (in the case of metal oxides) compared to the characteristic high intensity bands of the base matrix for the paint used. This aspect can also be observed from the analysis of the FTIR spectrum performed for the samples of additive paint with metallic fillers such as Al and Fe powder type (Figure 8, 9).

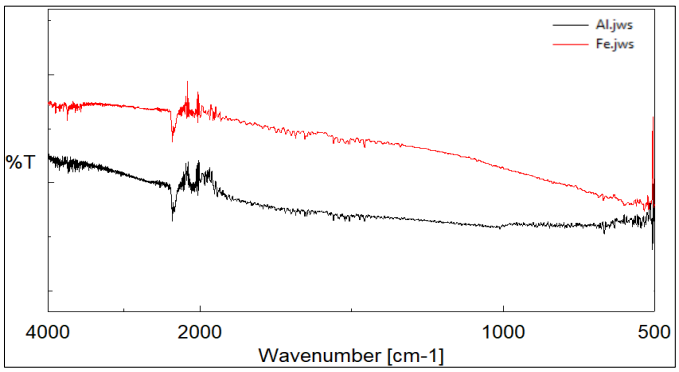

Figure 8. Recorded comparative ATR / FTIR spectra of metal nanopowder samples

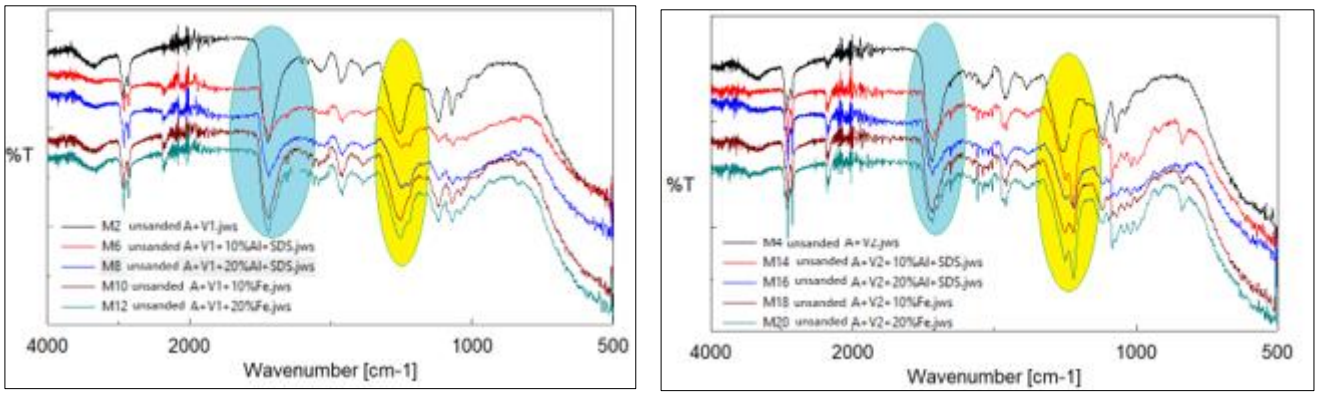

(a) (b)

Figure 9. Comparative ATR/FTIR spectra recorded for (a) V1 modified with different metal fillers and (b) V2 modified with different metal fillers

However, it should be noted that the addition of metal powders leads to a general change in the shape of the bands characteristic of groups C = O, in the region 1610-1780 cm^{-1} (band widens), respectively C-O-C, from 1258 cm^{-1} (band widens and acquires a multi-peak structure).

It can also be seen that the band characteristic of hydroxyl groups from 3390 cm^{-1} decreases in intensity with the addition of metal powder. This can be explained by the existence of (electrostatic) interactions between the basic acrylic paint matrix and the metal particles, possibly with the formation of hydrogen bonds with the surface of the metal particles [23, 24].

3.8. FTIR analysis conclusions

The ATR/FTIR spectra of the two samples are almost identical, suggesting that the two paints analyzed have the same basic chemical structure. Although there are color differences between the two paints, white (V1) and silver (V2), respectively, the ATR/FTIR spectrum of V2 has no additional bands to be attributed to the color pigment.

3.8. Analize DSC / DSC analysis

The DSC curves were recorded using Setaram 131 Evo equipment, France 2010, in non-isothermal mode (30-350°C) with a heating rate β = 10°C/min, in the oxidizing atmosphere (synthetic air with a flow rate of 50 mL/min). The mass of the samples was between 1.7 and 3.5 mg [25].

- Technical features:

The equipment can use a wide range of temperatures (-170 to 700°C) and is designed to analyze polymers and plastics (characterization, quality control), organic, pharmaceutical and inorganic products for both purity and stability, thermal loss, mass loss and the beginning of the decomposition process. The recorded curves were processed using Calisto Processing software, provided by the equipment manufacturer, to determine the characteristic parameters of the analyzed material: melting temperature (Tt), melting enthalpy (ΔHt), oxidation start temperature (OOT). The determination of these parameters was performed according to the procedure PL-MAV-36/2017.

The degree of crystallinity was determined using the following formula:

$$\chi_{cr} = \frac{\Delta H_t}{\Delta H_{t,100\%}\,(1-\Phi)}\,100 \qquad (2)$$

where:

- ΔHt is the melting enthalpy of the tested material;
- ΔHt, 100% melting enthalpy of 100% crystalline polymer;
- Φ is the weight fraction of metal particles in polymer composites.

DSC (differential scanning calorimetry) technique was used to characterize the polymeric materials in thermal regime. Thus, the degree of hardening of the coating film, the compatibility of the multiphase systems and the identification of the transitions occurred as a result of the aging of the polymeric material were measured.

The results obtained from the dielectric tests performed on the 16 additive systems showed that the samples with a maximum percentage (20%) of metal nanopowders show the highest values of electrical conductivity. The 4 non-additive EMs were subjected to UV radiation for 360 h and their behavior was studied by varying the dielectric characteristics. For each such non-additive system subjected to UV radiation, it was calculated the estimated remaining lifetime in case the exposure to UV radiation is continued. These estimations indicate that, for sample M2, the coating should be redone at the end of the exposure period (360 h) and for sample M1, after about 100 h after the exposure period. Thus, it was determined that the most affected by UV radiation is M2 and the most resistant to UV radiation is M4.

The ATR/FTIR spectra of the two paint samples analyzed showed that they were almost identical, suggesting that the paints tested had the same basic chemical structure. Although there are color differences between the two paints, white (V1) and silver (V2), respectively, the ATR/FTIR spectrum for V2 has no additional bands to be attributed to the pigment. This can be explained by the fact that the pigment used in V2 does not show IR absorption (such as metal powders), or the adsorption is very weak (in the case of metal oxides), and by comparison with the characteristic bands, of high intensity of the basic matrix paint. DSC analysis showed that pigment paint (V2) has low thermal oxidation stability and lower decomposition temperatures than V1. Therefore, V2 is less stable under usage conditions, under the influence of normal environmental factors (temperature, humidity, natural or artificial light, etc.) compared to V1.

Depending on the observed thermal effects and the temperatures at which they occur, the DSC curves can be divided into four main regions:

- 60-120°C - *water evaporation*. The DSC curves show a maximum endotherm in this region, due to the evaporation of traces of water from the paint composition. It can be seen that the temperature at which the evaporation process begins is lower for sample V2 (about 60°C) compared to V1 (about 90 °C). This phenomenon is similar to the one observed in the evaporation of water adsorbed on the surface of metal particles, in this case, being water adsorbed on the surface of the pigment (whose chemical nature is unknown, possibly inorganic in nature); Figure 10 shows the DSC thermograms recorded on the two paint samples analyzed. The mass of the samples analyzed by the DSC technique was between 2 and 4 mg. DSC analysis was performed on the initial paint samples.

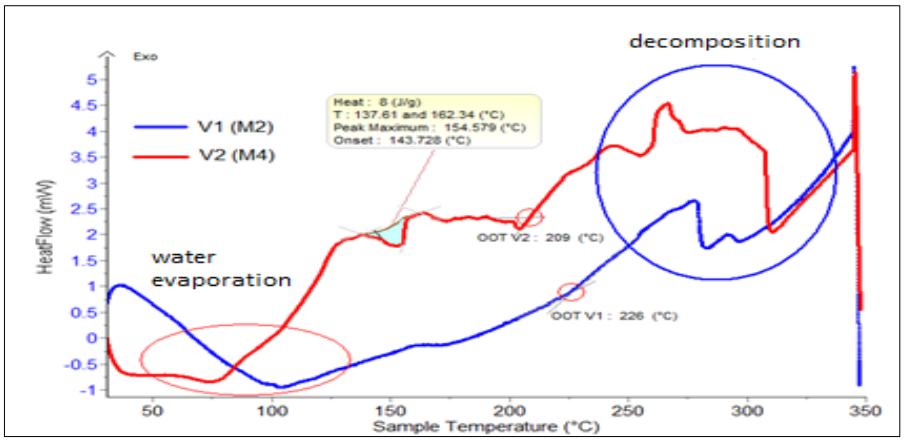

Figure 10. DSC curves recorded on the initial paint samples

-140-200°C. In this temperature range, the recorded DSC curves show notable differences between the two types of paints. V2 has a series of endothermic peaks, the largest being observed at about 155°C. These peaks may be due to the evaporation of volatile compounds introduced into the paint V2, as compatibilizing agents, as solubilizing or pigment stabilizing agents;

- 200-250°C. In this temperature range the process of oxidation of the organic matrix in the paint takes place; the higher the starting temperatures of this process, the higher the stability of the material is [23, 24, 25]. It can be seen that V2 has an OOT value of about 209°C, much lower than that of V1, whose OOT appears at 226°C. Thus, the paint V2 has a much lower stability than V1, due to the added color pigment which may have a pro-oxidant action;

- 250-350°C. This temperature range is associated with the thermooxidative decomposition of the paint. As with OOT values, the temperatures at which the decomposition process begins are much lower for V2 (242°C) compared to V1 (309°C). For both paints the process takes place in two stages, being determined, most likely, by the decomposition of different components in the structure of the paints.

4.Conclusions

Within this paper, 20 EM of Al/Fe paint/plastic/nanopowder systems type were made. Out of these, 4 MS were non-additive and 16 MS were additive. The addition was made to improve the way the paint is displayed on plastic substrates. After testing the additive, the SDS additive was chosen because it slightly increases the electrical conductivity of the samples. Al/Fe paint/plastic/nanopowder systems were obtained on unsanded substrates, degreased and mechanically cleaned before painting. These EMs thus obtained were characterized by dielectric tests and FTIR and DSC analyzes. Following these tests it can be concluded that from the point of view of:

- EM dielectric behavior, with the highest conductivity values are M11, M12, M19 and M20,

- resistance to the action of UV radiation, the most affected by UV radiation is M2 and the most resistant to UV radiation is M4,

- FTIR analyses, the two paints are almost identical, suggesting that the two paints analyzed have the same basic chemical structure, and the DSC analysis showed that the pigment paint (V2) has a stability to thermal oxidation and lower decomposition temperatures than V1.

Acknowledgments: This work was supported by the Romanian Ministry of Research, Innovation and Digitalization, project number 25PFE/30.12.2021 - Increasing R-D-I capacity for electrical engineering-specific materials and equipment with reference to electromobility and "green" technologies within PNCDI III, Programme 1, NANO-REV-EM-ASAM Project/Competitiveness Operational Programme 2014-2020, under grant ID P_37_757, cod my SMIS: 104089, nr. 119/16.09.2016 and the project 12 PTE/2020 - Equipment for the stimulation of biochemical processes in wastewater treatment plants – ESELFBIO; PN project no. 46N/2019.

References

1.***Ctr. Third Party Services no. 271/05.03.2021 "Physico-chemical characterization in laboratory conditions of compounds with the role of paints and primers, obtained by dispersing and stabilizing nano-additives with special electromagnetic properties in different solvents", 2021, Beneficiary MASKLOGIK SRL
2.***Ctr. Third Party Services no. 1505/11.10.2021 "Research services: characterization of the endurance of monolayer and multilayer coatings with paints and primers", 2021, Beneficiary MASKLOGIK SRL
3.PROGRAM 14 N/2016, Evaluation of the lifespan of polymeric protective films under the synergistic action of climatic stressors. Determination of remaining life for painted industrial systems in operation
4.SALOVARDA, M., MALARIC, K., Measurements of Electromagnetic Smog, *Electrotechnical Conference*, MELECON 2006. IEEE Mediterranean, 206, 470–473
5.URSAN, G.A., PLOPA, O., et al. Obtaining of the Paints with Electromagnetic Shielding Properties *International Conference on Electromechanical and Energy Systems*, 2021, 978-1-6654-0078-7/21/ $31.00. *IEEE* |DOI: 10.1109/SIELMEN53755.2021.9600281
6.***TDS Nr. 289 "OSKAR DIRECT PE MELAMINA & PLASTIC"
7.***https://nanografi.com/
8.CARAMITU, A.R., MITREA, S., et al., Dielectric Behavior and Morphostructural Characteristics of Some HDPE Composites/Metal Nanopowders, *Mater. Plast.*, **56**(1), 2019, 103-109
9.LEARNER, T., The use of a diamond cell for the FTIR characterisation of paints and varnishes available to twentieth century artists, IRUG2 Meeting, 1995, 7-20
10.DOLNÍK, B., Electromagnetic compatibility. (Elektromagnetická kompatibilita), *TU of Košice, monography*, 2013, ISBN 978-80-8086-221-3
11.BHAT, M.A., KUMAR, DR.V., Calculation of SAR and Measurement of Temperature Change of Human Head Due to the Mobile Phone Waves at Frequencies 900 MHz and 1800 MHz., *Advances in Physics Theories and Applicat*, **16**, 2013
12.SIVANI, S., SUDARSANAM, D., Impacts of radio-frequency electromagnetic field (RF-EMF) from cell phone towers and wireless devices on biosystem and ecosystem – a review, *Biology and Medicine*, **4**(4), 2012, 202–216, ISSN 0974-8369
13.OLMEDO, L., HOURQUEBIE, P., JOUSSE, F., *Handbook of organic conductive molecules and polymers*, New York: John Wiley and Sons, **3,** 1997
14.LEE, S.M., International Encyclopedia of Composites, New York: VHC Publishers 1991
15.FOLGUERAS, L.C., REZENDE, M.C., Multilayer radar absorbing material processing by using polymeric nonwoven and conducting polymer, *Material Research*, **11**(3), 2008, 245-249
16.CHANDRASEKHAR, P., *Conducting Polymers fundamentals and applications*, Boston: Kluwer Academic Publishers, 1999

17.***Handbook of Conducting Polymers, New York: Marcel Dekker, 1998
18.RUCK, G.T., BARRICK, D.E., et. al. Radar cross section handbook, New York: Plenum Press, **1**, 1970
19.NAITO, Y., Thickness of the ferrite absorbing wall, *Electronics and Communications in Japan*, **52**-B(1), 1970, 71-75
20.NAITO, Y, SUETAKE, K., Matching frequency of electromagnetic wave absorber utilizing ferrite, *Electronics and Communications in Japan*, **52**-B(7), 1970, 61-66
21.MUSAL, H.M., HAHN, H.T., Thin-layer electromagnetic absorber design, *IEEE Transactions on magnetics*, vol. **25**(5), 1989, 3851-3853
22.NICOLSON, M., ROSS, G., Measurement of the intrinsic properties of materials by time domain techniques, *IEEE Trasaction Instrum. Meas.*, **IM-19**, 1970, 377-382
23.***http://www.irug.org/documents/1Learner.pdf
24.ILIE, S., SETNESCU, R., LUNGULESCU, E.M., MARINESCU, V., ILIE, D., SETNESCU, T., MARES, G., Investigations of a mechanically failed cable insulation used in indoor conditions. *Polymer Testing*, **30**(2), 2011, 173-182
25.PINTUS, V., PLOEGER, R., CHIANTORE, O., WEI., S., SCHREINER, M., Thermal analysis of the interaction of inorganic pigments with p(nBA/MMA) acrylic emulsion before and after UV ageing. *Journal of Thermal Analysis and Calorimetry*, **114**(1), 2012, 33–43

Manuscript received: 23.03.2022